Nat. Hazards Earth Syst. Sci. Discuss., 3, 3509–3541, 2015
www.nat-hazards-earth-syst-sci-discuss.net/3/3509/2015/
doi:10.5194/nhessd-3-3509-2015


Natural Hazards and Earth System Sciences
Discussions
Open Access



# Debris flow susceptibility mapping using a qualitative heuristic method and Flow-R along the Yukon Alaska Highway Corridor, Canada

**A. Blais-Stevens and P. Behnia**

Geological Survey of Canada, 601 Booth Street, Ottawa, Ontario, K1A0E8, Canada

Received: 24 April 2015 – Accepted: 28 April 2015 – Published: 29 May 2015

Correspondence to: A. Blais-Stevens (ablais@nrcan.gc.ca)

Published by Copernicus Publications on behalf of the European Geosciences Union.







## Abstract

This research activity aimed at reducing risk to infrastructure, such as a proposed pipeline route roughly parallel to the Yukon Alaska Highway Corridor (YAHC) by filling geoscience knowledge gaps in geohazards. Hence, the Geological Survey of Canada compiled an inventory of landslides including debris flow deposits, which were subsequently used to validate two different debris flow susceptibility models. A qualitative heuristic debris flow susceptibility model was produced for the northern region of the YAHC, from Kluane Lake to the Alaska border, by integrating data layers with assigned weights and class ratings. These were slope angle, slope aspect (derived from a 5 m × 5 m DEM), surficial geology, permafrost distribution, and proximity to drainage system. Validation of the model was carried out by calculating a success rate curve which revealed a good correlation with the susceptibility model and the debris flow deposit inventory compiled from air photos, high resolution satellite imagery, and field verification. In addition, the quantitative Flow-R method was tested in order to define the potential source and debris flow susceptibility for the southern region of Kluane Lake, an area where documented debris flow events have blocked the highway in the past (e.g., 1988). Trial and error calculations were required for this method because there was not detailed information on the debris flows for the YAHC to allow us to define threshold values for some parameters when calculating source areas, spreading, and runout distance. Nevertheless, correlation with known documented events helped define these parameters and produce a map that captures most of the known events and displays debris flow susceptibility in other, usually smaller, steep channels that had not been previously documented.

## 1 Introduction

Over the past decades, there have been ongoing discussions about building a pipeline roughly parallel to the Yukon Alaska Highway Corridor, in northern Canada (YAHC;





NHESSD
3, 3509–3541, 2015



Fig. 1a). Portions of the proposed pipeline route intersect critical geological regions and areas prone to geological hazards, such as landslides, earthquakes due to active faults, subsidence from thermo-karstic erosion, and permafrost degradation. One of the roles of the Geological Survey of Canada (GSC), as part of Natural Resources Canada, is to reduce risk of geohazards to critical linear infrastructure, such as a proposed pipeline projects by providing baseline geoscience information to decision-makers.

The YAHC is roughly 875 km long and about 40 km wide and covers roughly 22 000 km$^2$ as it does not include the portions that extend into British Columbia (Fig. 1a). As a first step in assessing the types of geohazards, the GSC in collaboration with the Yukon Geological Survey (Huscroft et al., 2004), compiled an inventory of geological hazards, particularly landslides (Blais-Stevens et al., 2010a). Several landslide types were observed including debris flow deposits, debris slides, rockfalls, rock slides, active layer detachment slides, retrogressive thaw slumps, among others (Blais-Stevens et al., 2011). Once the baseline landslide information was compiled, the next step was to provide an overview of the landslide distribution and landslide "hot spots" by plotting distribution maps and producing regional qualitative landslide susceptibility maps (Blais-Stevens et al., 2010b, 2011, 2012, 2014; Couture et al., 2010). Different susceptibility models were created for different types of landslides, namely rockfall/rocks slides, active layer detachment slides, retrogressive thaw slumps, and debris flows.

Choosing which landslide susceptibility method depended on several factors. Some of the factors were scale, availability of geological and geomorphological data in digital format, software and hardware capabilities, and technical experience with GIS platform (Soeters and van Westen, 1996; van Westen et al., 2008). For the YAHC, we chose the simplest approach, a qualitative heuristic method as the study area was vast and uniform geological information was available at a broad scale. We modified and adapted the models first used for landslides triggered in permafrost along the Mackenzie Valley (Riopel et al., 2006) and for the Sea to Sky Highway in southern British Columbia (Blais-Stevens et al., 2012). Furthermore, previous studies revealed





NHESSD
3, 3509–3541, 2015



that debris flows along the Alaska Highway had occurred previously and blocked the highway, particularly in the south end of Kluane Lake (Evans and Clague, 1989; Lipovsky, 2005; Koch et al., 2014; Fig. 1c). Such an event occurred in 1988 following a torrential downpour; the highway was blocked by debris for seven days (Evans and Clague, 1989; Lipovsky, 2005). Therefore, with a higher precision Digital Elevation Model (DEM; 10 m × 10 m), we used a quantitative method using Flow-R to assess the potential source areas in steep channels and corresponding debris flow susceptibility (Horton et al., 2013) in the area where documented debris flows had occurred. Hence, the objectives of the paper are to (1) assess the regional debris flow susceptibility using a qualitative heuristic method for the northern portion of the corridor (Fig. 1b), (2) define the local potential source areas for debris flows and (3) model the debris flow susceptibility using the quantitative Flow-R method for the south end of Kluane Lake (Fig. 1c).

## 2 Physiographic setting and geology

The Yukon Alaska Highway Corridor traverses ten physiographic regions. From northwest to east in a broad sense, the relief varies from mountainous to rounded hills, to lowlands. The maximum elevation within the study area is 2799 m, located roughly southeast of the southernmost point of Kluane Lake and the minimum elevation, occurs about 15 km west of Haines Junction (Fig. 1b). Two major faults cut across the YAHC, namely the Denali and Tintina faults (Fig. 1a). For a detailed description of the physiographic regions, the reader is referred to Mathews (1996) and Huscroft et al. (2004).

The YAHC tectonic setting is largely the result of 190 million years of accretion of exotic terranes and intervening sediments onto the ancient North American continental plate (Gordey and Makepeace, 2003; Huscroft et al., 2004). Along the YAHC, from west to east, the Kluane ranges are composed of young sedimentary rocks (< 150 Ma old). Further east, felsic intrusions dominate within the Yukon Plateaus. Towards





NHESSD
3, 3509–3541, 2015



Whitehorse, Upper Cretaceous volcanic rocks and valley-filling Quaternary basalts are exposed. Within the Liard Lowland eastward, there are outcrops of Paleozoic sedimentary rocks (Gordey and Makepeace, 2003; Huscroft et al., 2004).

The abundance of surficial sediments along the YAHC is the result of several Quaternary glaciations. Hillslopes are covered by till blankets and veneer. Coarser ice-marginal meltwater deposits are commonly flanked along these hillslopes. In the steep mountainous terrain, weathered bedrock and reworked till form colluvium along valley sides. These are a major source for mass movement within the YAHC (Huscroft et al., 2004).

### 2.1 Climate and vegetation

The study area is characterized by a sub-arctic continental climate with long, cold winters, and short mild summers with low relative humidity and low to moderate precipitation averaging 340 mm per year. The mean temperatures vary from −27 °C in January to 27 °C in July (Huscroft et al., 2004). The YAHC lies within the Boreal Forest Ecozone, which is dominated by white and black spruce. Trembling aspen grows in meadows and open forests. The treeline varies between 1400 m in the east and 1200 m in the northwest corridor (Huscroft et al., 2004).

### 2.2 Permafrost

The YAHC is underlain by discontinuous permafrost. It mainly lies within the transition zone from sporadic discontinuous permafrost to extensive discontinuous permafrost (Heginbottom et al., 1995). At a broad scale, the distribution of ground ice along the highway ranges from 80 % north of Kluane Lake; < 50 % of the ground underlain by permafrost between Kluane Lake and Takhini River (~ 20 km west of Whitehorse); < 20 % from the Takhini River valley to just west of Teslin (~ 180 km east of Whitehorse); and < 5 % east of Teslin Lake (Fig. 1a); (Rampton et al., 1983; Huscroft et al., 2004). A higher resolution permafrost probability model (30 m × 30 m pixel) was published





NHESSD
3, 3509–3541, 2015



for Yukon by Bonnaventure et al. (2012). This probability distribution model broadly resembles previous permafrost distribution maps, but displays variation at a finer scale (Bonnaventure et al., 2012). This served as a data layer in the qualitative heuristic model.

## 3 Previous work

Landslide characterization and inventory compilation in the Yukon was carried out by Huscroft et al. (2004), Blais-Stevens et al. (2010a) published a regional landslide inventory based solely on air-photo interpretation (1960s–1990s air-photos from National Air-Photo Library) that also included the contribution by Huscroft et al. (2004). Interpretation of high resolution satellite imagery (WorldView-2) collected in 2010 helped fine tune and update the inventory that was used to validate regional landslide susceptibility models as well as field verification (Blais-Stevens et al., 2010b, 2011, 2012).

Debris flow modeling has been carried out by several researchers (e.g., Costa, 1984; Hungr et al., 1984; Berti and Simoni, 2007; Begueria et al., 2009; Hussin et al., 2012; Fischer et al., 2012; among many others). Horton et al. (2008, 2013) used a distributed empirical model that can be transposed to a small area within YAHC where inventory of past events exist. In addition to the qualitative heuristic method, the south portion of the Kluane Lake, an area adjacent to the Kluane Ranges (Fig. 1a–c) was a suitable area to test this method because (1) a high resolution DEM was available for this area, (2) the area has witnessed extreme debris flow events (July 1988), and (3) it contained several mapped debris flow deposits to validate the model.





NHESSD
3, 3509–3541, 2015



## 4 Susceptibility mapping methodology

### 4.1 Regional qualitative heuristic susceptibility mapping

The qualitative approach used for landslide susceptibility mapping is a simple heuristic approach modified from Soeters and van Westen (1996); Riopel et al. (2006); Blais-Stevens et al. (2012). Previous publications by Blais-Stevens et al. (2010b, 2011, 2012) demonstrated landslide susceptibility mapping for the entire corridor using a 30 m × 30 m DEM (Fig. 1a). In this study, the authors focused on the northern portion, more mountainous region of the corridor (Fig. 1b) and used a similar approach, but with a higher resolution DEM (5 m × 5 m produced by Natural Resources Canada's Centre for Geospatial Information, 2014). The simple equation is defined by a susceptibility index for debris flows in which the instability factors served as the variables. Each variable was assigned a percent weight based on expert knowledge according to its importance in slope instability. The factors of instability were derived from the available geological maps or were generated from DEM as data layers and consequently reclassified. Classes within each parameter were also assigned a weight based on their potential contribution to slope failure. The resulting parametric equation is the sum of all variables and represents a susceptibility index (SI) ranging between 0 and 1 for each pixel (5 m × 5 m). The heuristic modelling was carried out independently of the debris flow deposit inventory where it was later used to validate the susceptibility map. The criteria considered relevant to initiation of debris flows in the study area include slope angle, slope aspect sediment type, proximity to drainage system, and permafrost distribution. Slope angle is an important factor in initiation of a debris flow. According to Ortigao and Kanji (2004), the minimum slope angles reported in the literature are above 20–25°. There is an increase in the number of debris flows as the slope angle increases. At slope angles higher than 34–37°, there is a decrease because of the existence of rock scarps (Ortigao and Kanji, 2004). Similarly, Dai and Lee (2001) noted that at slope gradients ≥ 40°, the slope forming material of the terrain is composed of weathered rock which is stronger and less prone to failure than colluvium. The slope





NHESSD
3, 3509–3541, 2015



map was generated from a 5 m × 5 m DEM and was reclassified into five classes and assigned the highest rating to slope angles ranging from 25 to 45° (Table 1). Sediment availability is another important factor in initiation of debris flows. The surficial geology map (Yukon Geological Survey, 2014) was reclassified into six classes based on the favourability of the sediments in developing debris and were rated accordingly. The drainage map was considered equally important as slope angle, as debris flows are usually triggered in steep streams. This data layer was generated by creating five buffer zones around the drainage system. Each zone was rated based on its proximity to drainage system (Table 1). Permafrost probability distribution was also considered as a factor contributing to slope instability given the potentially high distribution in the mountains where most debris flows are initiated. This data layer was extracted from the permafrost probability distribution model generated for southern Yukon and northern British Columbia (Bonnaventure et al., 2012). The probability map was reclassified into 10 classes and was rated based on the probability of permafrost occurrence (Table 1). We also considered the direction of slope, i.e., the slope aspect as a potential contributing factor, but to a lesser degree than the other data layers because of the potential for south facing slope being more exposed to solar radiation, which in turn, would contribute to either increased snow melt or permafrost thaw and subsequently to the drainage system. The slope aspect map, also generated from the 5 m × 5 m DEM was reclassified into five classes with the highest ratings assigned to slopes facing SE to SW (Table 1). All geological information was compiled and processed on an ArcGIS platform (v. 10.2.2).

Once the parameter maps were reclassified and rated, they were integrated using the following equation:

$$\mathrm{SI} = 0.3D + 0.3S1 + 0.2G + 0.15P + 0.05S2, \quad (1)$$

where $D$ is proximity to drainage system, $S1$ is the slope angle, $G$ is the type of surficial geology deposit, $P$ is the permafrost distribution, and $S2$ is the slope aspect. The resulting debris flow susceptibility map (Fig. 2) shows a susceptibility index ranging





NHESSD
3, 3509–3541, 2015



from 0 to 1 in which the high values are the areas of high susceptibility (shown in red). Although the highly susceptible areas are dominant in the most western region of the corridor, there are areas of high susceptibility found close to the highway, near Kluane Lake.

We used the mapped debris flow inventory consisting of 306 deposits to evaluate the debris flow susceptibility map. Given that the inventory only includes the deposits and not the initiation zones, we made the assumption that the source area likely occurs within at least 500 m distance uphill from the apex of the deposit. To delineate the potential source area (initiation zone), the stream network was extracted from the flow accumulation map and catchment basins were created for the apex of each debris flow deposit. Areas 100 m around the streams were selected and were intersected with the catchment basins. The areas covered by both catchment basins and streams within 500 m upstream from the debris flow deposits were selected as potential source areas (Fig. 5) where the maximum susceptibility value occurring within each polygon was compiled. A success rate of prediction curve was generated by plotting the cumulative percentage area from high to low susceptibility against the cumulative percentage of debris flow sources predicted (Chung and Fabbri, 2003). The qualitative heuristic susceptibility map shows a high prediction rate with respect to debris flow source areas (Fig. 3). About 80 and 90 % of the debris flow sources are predicted within the top 10.74 and 13.57 % of high susceptibility areas, respectively.

### 4.2 Quantitative susceptibility mapping

We used Flow-R model developed by Horton et al. (2008, 2013) to assess debris flow susceptibility and focus on a smaller area of the YAHC at the south end of Kluane Lake. Flow-R, developed under Matlab® by Horton et al. (2013) stands for *Flow path assessment of gravitational hazards at a Regional scale* and was downloaded from www.flow-r.org. The main dataset required for susceptibility assessment in Flow-R is a grid based DEM. The quality of DEM is of great importance for the accuracy of the results. We used a 5 m × 5 m DEM and resampled it to 10 m in order to reduce





NHESSD
3, 3509–3541, 2015



the roughness and avoid the effect of channelization that can occur with very high resolution data. The following concepts of Flow-R and the implemented models are summarized from Horton et al. (2013). Susceptibility assessment using Flow-R involves two stages:

Step 1 – Delineation of debris flow source areas based on the geological, morphological and hydrological criteria critical in debris flow occurrence. These controlling parameters are used in grid format and are classified according to their favourability in debris flow initiation. The dataset are classified as favorable, if initiation is possible, excluded if the initiation is unlikely and ignored if there is not enough evidence in favourability of the class. The classified input parameters are integrated based on the following rule: a grid cell is considered a source area if it was classified as favorable at least in one of the parameter maps, but was never classified as excluded (Horton et al., 2013).

Step 2 – Propagation of the source areas. The potential source areas are propagated using two types of algorithms: (1) spreading algorithms which determine the path and the way debris flows spread and (2) algorithms which are based on the friction laws and control the runout distance of debris (Horton et al., 2013).

The spreading algorithms address flow direction algorithms and persistence functions and describe downslope movement of material. Various methods have been proposed in the literature for single and multiple flow directions, such as O'Callaghan and Mark (1984); Freeman (1991); Quinn et al. (1991); Costa-Cabral and Burges (1994); and Tarboton (1997). In single flow direction methods, it is assumed that material moving downslope follow only the steepest downslope direction. Multiple flow direction methods assume that flow occurs in all downslope directions from a given point. In grid based elevation models, the proportion of flow each downslope cell receives from the central cell is weighted according to the slope gradient between the downslope cell and the central cell. Holmgren (1994) adjusted the weights in multiple flow direction algorithm by adding a variable exponent $x$ to control the divergence





NHESSD
3, 3509–3541, 2015



(Eq. 2):

$$P_i^{\mathrm{fd}} = \frac{(\tan\beta_i)^x}{\sum_j^8 (\tan\beta_j)^x} \forall \begin{cases} \tan\beta > 0 \\ x \in [1; +\infty[, \end{cases} \quad (2)$$

where *i, j* are flow directions, $P_i^{\mathrm{fd}}$ is flow proportion in direction $i$, $\tan\beta i$ is the slope gradient between the cell in direction $i$ and the central cell and $x$ is the variable exponent. With $x = 1$ the algorithm corresponds with multiple flow direction used by Quinn et al. (1991) and the distribution would be the same as a single flow direction distribution when $x \to \infty$ (Holmgren, 1994). Horton et al. (2013) added a height factor to Holmgren's algorithm in order to smooth the roughness of the DEM and obtain a more consistent spreading. In this modified version, the height of the central cell is changed by a factor *dh*, which in turn, results in the change of gradient values. Another influencing factor which is implemented in Flow-R is inertial parameter. The flow direction is weighted based on the change in direction according to the persistence function (Eq. 3, Gamma, 2000 in Horton et al., 2013):

$$P_i^{\mathrm{p}} = w_{\alpha(i)}, \quad (3)$$

where $P_i^{\mathrm{p}}$ is the flow proportion in direction $i$, and $\alpha(i)$ is the angle between previous direction and the direction from central cell to cell $i$. Three implementations of weights have been proposed by Horton et al. (2013) namely proportional, cosine, and the one based on Gamma (2000). The weights resulted from the persistence function and those from flow direction are combined to provide the overall susceptibility according to Eq. (4) (Horton et al., 2013).

$$P_i = \frac{P_i^{\mathrm{fd}} P_i^{\mathrm{p}}}{\sum_{j=1}^{8} P_j^{\mathrm{fd}} P_j^{\mathrm{p}}} P_0, \quad (4)$$





NHESSD
3, 3509–3541, 2015



where $i$, $j$ are flow directions, $P_i$ is the susceptibility value in direction $i$, $p_i^{fd}$ is the flow proportion according to the flow direction algorithm, $p_i^{p}$ the flow proportion according to the persistence and $p_0$ the previously determined susceptibility value of the central cell.

The runout distance is estimated by an energy balance established between the central cell and the cell in direction $i$, based on simple friction laws (Eq. 5).

$$E_{kin}^{i} = E_{kin}^{0} + \Delta E_{pot}^{i} - E_{f}^{i}, \quad (5)$$

where $E_{kin}^{i}$ is the kinetic energy of the cell in direction $i$, $E_{kin}^{0}$ is the kinetic energy at the central cell, $\Delta E_{pot}^{i}$ is the change of potential energy to the cell in direction $i$. and $E_{f}^{i}$ is the energy loss due to friction at the cell in direction $i$ (Horton et al., 2013). The runout distance algorithms control the distance which can be reached by debris flows. Two types of algorithms are available in Flow-R to assess the friction loss: a two parameter friction model based on Perla et al. (1980) and a simplified friction model based on maximum possible runout distance.

The Perla model originally proposed for snow avalanche motion, is based on a non-linear friction law and calculates the velocity of the flow at the end of segment $i$. The model requires the value of friction coefficient $\mu$ and mass-to-drag ratio $\omega$ to be provided (Eq. 6):

$$V_i = \left(a_i \omega (1 - \exp b_i) + V_0^2 \exp b_i\right)^{\frac{1}{2}}, \quad (6)$$

where $a_i = g(\sin\beta_i - \mu\cos\beta_i)$, $b_i = -2L_i/\omega$, $\mu$ is the friction parameter, $\omega$ is the mass to drag ratio, $\beta_i$ is the slope angle of the segment, $V$ is the velocity at the beginning of the segment, $L_i$ is the length of segment and $g$ is the acceleration due to gravity.

The simplified friction-limited model only requires the value of minimum travel angle (or angle of reach) which is the angle of line between the source and the end point of debris flow (Eq. 7):

$$E_i^{f} = g\Delta x \tan\varphi, \quad (7)$$





NHESSD
3, 3509–3541, 2015



where $E_i^f$ is the energy lost in friction from central cell to the cell in direction $i$, $\Delta x$ is the increment of horizontal displacement, $\tan \varphi$ is the gradient of energy line, and $g$ is the acceleration due to gravity (Horton et al., 2013). In order to keep the energy within reasonable values, a maximum threshold is introduced to avoid achieving unrealistic velocities in both models.

#### 4.2.1 Flow-R application to south Kluane Lake, Yukon Alaska Highway Corridor

**Source area delineation**

In order to delineate the source areas in the study area, we considered slope angle and curvature as the morphological factors, upslope contributing area as the hydrological factor, and surficial geology as the lithological factor.

Slope angles above 20–25° are reported by Ortigao and Kanji (2004) for initiation of most debris flows in the literature. According to Takahashi (1981) and Rickenmann and Zimmermann (1993), most debris flows occur at slope angles higher than 15° (Horton et al., 2013). We considered this value as the lower initiation slope angle in this study area.

The plan curvature was used to identify the concave curvatures as possible source areas based on the assumption that debris flows tend to occur in gullies where the curvature is concave. There is no established threshold value for curvature in the literature. Horton et al. (2013) used a curvature of $-2/100\,\mathrm{m}^{-1}$ based on a 10 m DEM, and analysis of orthophotographs in Switzerland. Fischer et al. (2012) used values from $-1.5/100$ to $-0.5/100\,\mathrm{m}^{-1}$ for debris flow susceptibility mapping in Norway and Park et al. (2013) used curvature values from $-2/100$ to $-1/100\,\mathrm{m}^{-1}$ for debris flow hazard zonation analysis in Korea. In order to establish a proper curvature threshold for the study area, we tested two threshold values of $-1.5/100$ and $-0.1/100\,\mathrm{m}^{-1}$ to select the favorable source areas. The selected source areas and their resulting propagation areas were examined using the mapped debris flow deposits of the study area. Most of the mapped debris flow deposits were captured by the propagation area in both





NHESSD
3, 3509–3541, 2015



cases, but the threshold value of $-0.1/100\,\mathrm{m}^{-1}$ provided a better agreement and could capture more debris flow deposits (Fig. 4).

Water, commonly as infiltration of rainfall or convergence of ground water into the soil, contributes to instability of steep slopes by increasing the soil weight and decreasing the soil strength (Savage and Baun, 2005). To estimate the water input, the flow accumulation which represents the upslope contributing area was used. Based on the analysis of past debris flow events, a relationship could be established between the upslope contributing area and slope. Horton et al. (2008, 2013) defined two curves for identifying the lower limit of debris flow initiation in central Alps. The first curve is based on the work of Heinimann et al. (1998 in Horton, 2013); and is considered as rare events. The second curve is based on the work of Rickenmann and Zimmermann (1993) on the extraordinary 1987 event in Switzerland. The threshold values for rare and extreme events are given in Eqs. (8) and (9) respectively (Horton et al., 2008, 2013).

$$\begin{cases} \tan\beta_{\mathrm{thres}} = 0.32 S_{\mathrm{uca}}^{-0.2} & \text{if } S_{\mathrm{uca}} < 2.5\,\mathrm{km}^2 \\ \tan\beta_{\mathrm{thres}} = 0.26 & \text{if } S_{\mathrm{uca}} \geq 2.5\,\mathrm{km}^2 \end{cases} \quad (8)$$

$$\begin{cases} \tan\beta_{\mathrm{thres}} = 0.31 S_{\mathrm{uca}}^{-0.15} & \text{if } S_{\mathrm{uca}} < 2.5\,\mathrm{km}^2 \\ \tan\beta_{\mathrm{thres}} = 0.26 & \text{if } S_{\mathrm{uca}} \geq 2.5\,\mathrm{km}^2 \end{cases} \quad (9)$$

where $\tan\beta_{\mathrm{thres}}$ is the slope threshold, and $S_{\mathrm{uca}}$ is the surface of the upslope contributing area. The main difference between the rare and extreme events occurs for the small catchments with areas between 1 and 10 ha. Thus, using the rare events limit would cause the omission of some potential sources, which are small but still can contribute to a debris flow event (Horton et al., 2008). In order not to miss any potential source area, we decided to use the extreme events limit. Furthermore, comparing the mapped debris flow deposits in the study area with the source areas created using both threshold values (Eqs. 8 and 9) showed that the extreme events limit is more consistent with the past debris flow events along the Yukon Alaska Highway area.





NHESSD
3, 3509–3541, 2015



The surficial geology deposits were classified into favorable, excluded, and ignored based on the type of surficial unit and suitability as being a source for sediments and debris material. The colluvium, till, and the drift units were classified as favorable, the organic material as excluded, and the rest of units as ignored. Once the parameter maps were classified, they were integrated to create the final source areas (Fig. 5).

## Susceptibility assessment

In order to calculate the potential spread from source areas, we used Holmgren (1994)'s method and its modified version as the flow direction algorithms (Horton et al., 2013). Using $\Delta h$ equal to 1 and 2 m provided somewhat more lateral spreading, except for a few debris flow fans, the effect was not very significant. This was expected for a 10 m DEM because the change of $\Delta h$ affects mainly the finer resolution DEMs (Horton et al., 2013). Holmgren (1994) proposed the value of exponent $x$ in the range of 4–6 and Claessens et al. (2005) suggested the value of 4 for debris flows. We applied the value of 4 in most of our simulations and compared the spreading results with the mapped debris flow deposits in the study area. The exponent values equal to 5 and 6 were also tested. These propagation results were not as satisfactory as with $x$ equal 4. Therefore, we selected the value of 4 for the rest of the simulations. To set the inertial algorithm which weights the flow proportion based on the persistence function for each direction change ($w$), we selected the proportional approach which assigns the weights of 1, 0.8, 0.4, 0, and 0, for $w$, $w_{45}$, $w_{90}$, $w_{135}$, and $w_{180}$, respectively.

Perla's (1980) two parameter friction model was used for the assessment of runout distance. Because there was no information on the mass-to-drag ratio $\omega$ and friction coefficient $\mu$ for the debris flow deposits in the study area, it was decided to calibrate these values by comparing the propagation areas resulting from different sets of $\omega$ and $\mu$ and the mapped debris flow deposits, while keeping the spreading parameters fixed. The tested values range from 10 to 1000 for $\omega$ and 0.01 to 0.3 for $\mu$. The resulting simulations using varying sets of $\omega$ and $\mu$ yield almost similar propagation for most of the debris flow deposits except for the relatively larger ones (Figs. 6 and





NHESSD
3, 3509–3541, 2015



7). With $\omega$ equal to 10 and $\mu$ equal to 0.3, only one very small debris flow deposit was completely reached in runout distance. About 69 % of the mapped debris flow deposits were completely or partly reached when $\omega$ equal to 20 and $\mu$ equal to 0.02 were used. Most of the debris flow deposits with the exception of two very large and three relatively large fans were reached with $\omega$ = 200 and $\mu$ = 0.06. The same result was also achieved with other sets of $\omega$ and $\mu$ (e.g., $\omega$ = 150 and $\mu$ = 0.05, $\omega$ = 100 and $\mu$ = 0.04). The best fit for the three relatively larger fans (A, B, and C in Fig. 6) were achieved with $\omega$ = 150 and $\mu$ = 0.02 because it provided a better fit for these fans, but did not change the propagation pattern for the rest of debris flow deposits (Fig. 6). Of the two very large fans, one is part of a larger fan located in the northwestern edge of the study area (A in Fig. 6) with only a very small portion reached in one area. The source area for this fan is likely located outside of the limit of the study area. The other very large fan, located southwest of Kluane Lake (E in Figs. 6 and 7), is just partly reached when $\omega$ greater than 600 at $\mu$ equal to 0.02 (or $\omega$ greater than 100 at $\mu$ = 0.01) are used (Fig. 7). Further increasing the mass-to-drag ratio mainly affects the runout distance for fans C, D, and E and a few channels in the east and north-east of the study area and does not change the propagation pattern for the rest of area (Figs. 6 and 7). Figure 7 displays correlation with the mapped debris flow deposits (Blais-Stevens, 2010a), but also the ones studied in detail by Koch et al. (2014) and those that were documented after the 1988 event (Evans and Clague, 1989; Lipovsky, 2005). Testing various sets of $\omega$ and $\mu$ showed that the runout distance was more sensitive to the friction coefficient rather than mass-to-drag ratio changes, particularly at higher values of $\mu$.

## Evaluation

The debris flow susceptibility map created using the propagation of source areas correlates well with mapped debris flow deposits. Out of 49 debris flow deposits, most are reached in terms of runout distance, but as discussed earlier, some of them are not completely covered in terms of lateral spreading. This is expected as many of these debris fans have been building since deglacial time (Koch et al., 2014) and are





NHESSD
3, 3509–3541, 2015



products of several events over time. Nevertheless, debris can still flow, propagate, and block the highway even as relatively small fans (Evans and Clague, 1989).

Debris flows triggered by heavy rains in 1988 and 1967 (B, F, G, and H in Figs. 7 and 8) are also used to evaluate the debris flow susceptibility map. Figure 8 displays WorldView2 images overlaid by the susceptibility map at the location of these events. Williscroft Creek watershed (Figs. 7 and. 8a) is a typical active fan along the foot of the Kluane Range (Evans and Clague, 1989) in which the highway was severed at B during heavy rains in July 1988. About 3.5 km north of Slims River (Fig. 7), two debris flows occurred in Holocene colluvium one of which blocked the highway at F (Figs. 7, 8b and 9). Another debris flow occurred about 1.5 km east of Slims River (G in Figs. 7 and 8c) and covered more than 500 m of the highway (Evans and Clague, 1989). A debris flow triggered by heavy rains during the summer of 1967 (location H in Figs. 7 and 8c) also blocked the highway. All four locations where the highway was severed, are covered by the propagation pattern in the debris flow susceptibility map created using Flow-R. The Williscroft Creek watershed is mainly covered in the middle part, but also is reached at B where the highway was blocked.

Koch et al. (2014) studied 30 large debris flow deposits along the YAHC between Beaver Creek and the south end of Kluane Lake using dendrochronology and tephrochronology to evaluate the potential hazard of debris flows on the highway. A number of 15 debris flow deposits lie in the south end of Kluane Lake (red dots in Fig. 8). Three of them coincide with the 1988 debris flow events documented by Evans and Clague (1989). All, except one of these fans, are captured by the propagation of source areas established using Flow-R. The susceptibility map also shows some areas for debris flow deposition that were not outlined as debris lobes in the inventory or other sources. These in some cases extend passed the highway (e.g., debris flow I in Figs. 7 and 8d.)





NHESSD
3, 3509–3541, 2015



## 5 Conclusion

Two separate methods were used to assess the debris flow susceptibility in the YAHC focussing on the northern portion of the corridor for the qualitative heuristic method and the south end of Kluane Lake for the quantitative method using Flow-R.

The qualitative method was based on expert knowledge using geological and geomorphological data layers with assigned weights and class ratings. The resulting susceptibility map displayed the steep channels as high susceptibility zones for potentially initiating debris flows (Fig. 2). For the most part, downstream from the high susceptibility zones, where the lower susceptibility zones are identified, is where the mapped debris flow deposits are found. Validation was carried out using 306 debris flow deposits and their source area estimated within 500 m upstream from the apex of the deposits. A success rate curve demonstrated that about 80 and 90 % of the debris flow sources were predicted within 10.74 and 13.57 % of high susceptible areas, respectively. In the southern portion of Kluane Lake, where 1988 debris flows deposits were documented (Evans and Clague, 1989) and studied in detail (Koch et al., 2014), the susceptibility zones upstream from the location of these deposits are high.

A quantitative approach for debris flow susceptibility focussed on a smaller area within the YAHC, at the southern end of Kluane Lake, where historical and pre-historic events had been documented. The Flow-R method (Horton et al., 2013) allowed us to quantitatively determine the potential source areas and also calculate potential spreading and runout. Trial and error calculations were needed during the modeling because there was not detailed information on the debris flow deposits to calculate threshold values for parameters controlling source area delineation, spreading and runout distance assessment. Nevertheless, correlation with known documented events helped us define these parameters and produce a map that captures most of the known events and displays debris flow susceptibility in other steep channels (Figs. 6 and 7). Applying Flow-R method for a large area with varied topography, i.e., using the same threshold values for the whole area, may result in overgeneralization in some areas.





NHESSD
3, 3509–3541, 2015



However, except the area southeast of Kluane Lake, which is characterized by a flatter topography, the rest of study area has a similar topography. Besides, using a wide range of values for parameters controlling spreading and runout distance did not change the propagation pattern dramatically, except for a few large and relatively large debris flow deposits.

The debris flow susceptibility map correlates well with known events and has also displayed other potential channels that could be susceptible to debris flows. The correlation with known events may or may not exactly match with the size of the mapped debris flow deposits. This is expected as some of these debris flow fans have been building since deglaciation time.

*Acknowledgements.* This project was funded by Natural Resources Canada's Program of Energy and Research and Development. The authors would like to thank Sharon Smith (Geological Survey of Canada project leader), Panya Lipovsky (Yukon Geological Survey), and John Clague (Simon Fraser University) for their continual input. Pascal Horton (Terr@num Ltd) is acknowledged for his advice, comments and suggestions. Crystal Huscroft (Thompson River University) is thanked for the photo of Horseshoe Bay. Amaris Page, Marian Kremer, Ariane Castagner, and Joe Koch are acknowledged for their technical assistance. Jeff Harris (Geological Survey of Canada) is also thanked for his comments and suggestions. Pierre Gravel and his colleagues (Canadian Centre for Geospatial Information) are thanked for providing a new high resolution DEM.

## References

Beguería, S., Van Asch, Th. W. J., Malet, J.-P., and Gröndahl, S.: A GIS-based numerical model for simulating the kinematics of mud and debris flows over complex terrain, Nat. Hazards Earth Syst. Sci., 9, 1897–1909, doi:10.5194/nhess-9-1897-2009, 2009.

Berti, M. and Simoni, A.: Prediction of debris flow inundation areas using empirical mobility relationships, Geomorphology, 90, 144–161, 2007.

Blais-Stevens, A., Couture, R., and Page, A.: Landslide inventory along the Alaska Highway Corridor, Yukon, Open File 6654, DVD, Geol. Surv. of Can., Ottawa, Ont., 2010a.





NHESSD

3, 3509–3541, 2015



Blais-Stevens, A., Couture, R., Page, A., Koch, J., Clague, J. J., and Lipovsky, P.: Landslide susceptibility, hazard and risk assessments along pipeline corridors in Canada, in: Proceedings of the 63rd Canadian Geotechnical Conference and 6th Canadian Permafrost Conference, 12–16 September, 2010 Calgary (AB), 878–885, 2010b.

Blais-Stevens, A., Lipovsky, P., Kremer, M., Couture, R., and Page, A.: Landslide inventory and susceptibility mapping for a proposed pipeline route, Yukon Alaska Highway Corridor, in: Proceedings of the Second World Landslide Forum, Rome, Italy, 362, (ESS Cont. #20110101), 2011.

Blais-Stevens, A., Lipovsky, P., Kremer, M., Couture, R., and Smith, S.: Landslide inventory and susceptibility mapping for the Yukon Alaska Highway Corridor, in: Proceedings of the 11th International and 2nd North American Symposium on landslides and engineered slopes, 3–8 June 2012, Banff, Alberta, 1, 777–782, 2012.

Blais-Stevens, A., Kremer, M., Bonnaventure, P. P., Smith, S. L., Lipovsky, P., and Lewkowicz, A. G.: Active layer detachment slides and retrogressive thaw slumps susceptibility mapping for present-day and projected climate conditions along the Yukon Alaska Highway Corridor – a qualitative heuristic approach, in: Proceedings of the Engeneering Geology for Society and Territory, IAEG conference, (GSC Contribution: 20130369), 15–19 September 2014, Torino, Springer, 1, 449–453, 2014.

Bonnaventure, P. P., Lewkowicz, A. G., Kremer, M., and Sawada, M. C.: A Permafrost probability model for the southern Yukon and northern British Columbia, Canada, Permafrost. Periglac., 23, 52–68, doi:10.1002/ppp.1733, 2012.

Carson, M. A. and Kirkby, M. J.: Hillslope Form and Process, Cambridge University Press, London, 475 pp., 1972.

Chung, C.-J. F. and Fabbri, A. E.: Validation of spatial prediction models for landslide hazard mapping, Nat. Hazards, 30, 451–472, doi:10.1023/B:NHAZ.0000007172.62651.2b, 2003.

Claessens, L., Heuvelink, G. B. M., Schoorl, J. M., and Veldkamp, A.: DEM resolution effects on shallow landslide hazard and soil redistribution modelling, Earth Surf. Proc. Land., 30, 461–477, doi:10.1002/esp.1155, 2005.

Costa, J. E.: Physical geomorphology of debris flows, in: Developments and Applications of Geomorphology, edited by: Costa, J. E. and Fleisher, P. J., Springer-Verlag, Berlin, 268–317, 1984.





NHESSD

3, 3509–3541, 2015



Costa-Cabral, M. C. and Burges, S. J.: Digital elevation model networks (DEMON): a model of flow over hillslopes for computation of contributing and dispersal areas, Water Resour. Res., 30, 1681–1692, 1994.

Couture, R., Blais-Stevens, A., Page, A., Koch, J., Clague, J. J., and Lipovsky, P. S.: Landslide susceptibility, hazard and risk assessment along pipelines in Canada, in: Proceedings of the 11th International Association for Engeneering Geology and the Environment Congress, edited by: Williams, A. L., Pinches, G. M., Chin, C. Y., McMorran, T. J., and Massey, C. I., Auckland, New Zealand, 5–10 September, 1023–1031, 2010.

Dai, F. C. and Lee, C. F.: Terrain-based mapping of landslide susceptibility using a geographical information system: a case study, Can. Geotech. J., 38, 911–923, doi:10.1139/t01-021, 2001.

Evans, S. G. and Clague, J. J.: Rain-induced landslides in the Canadian Cordillera, July 1988, Geosci. Can., 16, 3, 193–200, 1989.

Fischer, L., Rubensdotter, L., Sletten, K., Stalsberg, K., Melchiorre, C., Horton, P., and Jaboyedoff, M.: Debris flow modeling for susceptibility mapping at regional to national scale in Norway, in: Proceedings of the 11th International and 2nd North American Symposium on Landslides, Banff, Alberta, Canada, 3–8 June 2012, 723–729, 2012.

Freeman, T. G.: Calculating catchment area with divergent flow based on a regular grid, Comput. Geosci., 17, 413–422, doi:10.1016/0098-3004(91)90048-I, 1991.

Gamma, P.: dfwalk – Ein Murgang-Simulationsprogramm zur Gefahrenzonierung, Geographisches Institut der Universität Bern, Bern, Switzerland, 2000.

Gordey, S. P. and Makepeace, A. J.: Yukon digital geology, version 2.0 Geol. Surv. of Can., Ottawa, Ont., Open File 1749 and Open File 2003-9(D), 2 CD-ROMS, Yukon Geol. Surv., Whitehorse, Yukon, 2003.

Heginbottom, J. A., Dubreuil, M. A., and Harker, P. A.: Canada-Permafrost, in: National Atlas of Canada, 5th edn., National Atlas Information Service, Nat. Res. Canada, Ottawa, MCR4177, 1995.

Heinimann, H. R., Hollenstein, K., Kienholz, H., Krummenacher, K. B., and Mani, P.: Methoden zur Analyse und Bewertung von Naturgefahren, Bundesamt für Umwelt, Wald und Landschaft (BUWAL), Bern, Switzerland, 85, 247 pp., 1998.

Holmgren, P.: Multiple flow direction algorithms for runoff modelling in grid based elevation models: an empirical evaluation, Hydrol. Process., 8, 327–334, doi:10.1002/hyp.3360080405, 1994.





NHESSD

3, 3509–3541, 2015



Horton, P., Jaboyedoff, M., and Bardou, E.: Debris flow susceptibility mapping at a regional scale, in: Proceedings of the 4th Canadian Conference on Geohazards, 20–24 May 2008, Québec, Canada, 2008, 399–406, 2008.
Horton, P., Jaboyedoff, M., Rudaz, B., and Zimmermann, M.: Flow-R, a model for susceptibility mapping of debris flows and other gravitational hazards at a regional scale, Nat. Hazards Earth Syst. Sci., 13, 869–885, doi:10.5194/nhess-13-869-2013, 2013.
Hungr, O., Morgan, G. C., and Kellerhals, R.: Quantitative analysis of debris torrent hazards for design of remedial measures, Can. Geotech. J., 21, 663–677, 1984.
Huscroft, C. A., Lipovsky, P. S., and Bond, J. D.: A regional characterization of landslides in the Alaska Highway corridor, Yukon, Open File Rep. 2004–18, Yukon Geol. Surv., Whitehorse, Yukon, 65 pp., 2004.
Hussin, H. Y., Quan Luna, B., van Westen, C. J., Christen, M., Malet, J.-P., and van Asch, Th. W. J.: Parameterization of a numerical 2-D debris flow model with entrainment: a case study of the Faucon catchment, Southern French Alps, Nat. Hazards Earth Syst. Sci., 12, 3075–3090, doi:10.5194/nhess-12-3075-2012, 2012.
Koch, J., Clague, J. J., and Blais-Stevens, A.: Debris flow chronology and potential hazard along the Alaska Highway in southwest Yukon Territory, Environ. Eng. Geosci., 25–43, 2014.
Lipovsky, P. S.: Rapid landscape change and human response in the Arctic and sub-Arctic, an interdisciplinary conference, Field guide, Yukon College, Whitehorse, Yukon, 43–101, 2005.
Mathews, W. H.: Physiographic map of the Canadian Cordillera, 1 : 5 000 000 scale, Geol. Surv. of Can., Ottawa, Ont., 1986.
O'Callaghan, J. F. and Mark, D. M.: The extraction of drainage networks from digital elevation data, Comput. Vision Graph., 28, 328–344, doi:10.1016/S0734-189X(84)80011-0, 1984.
Ortigao, J. A. R. and Kanji, M. A.: Landslide classification and risk management, in: Handbook of Slope Stabilization, edited by: Oritgao, J. A. R. and Sayao, A. S. F. J., Springer Verlag, Heidelberg, 27–66, 2004.
Park, D., Lee, S, Nikhil, N. V., Kang, S., Park, J.: Debris flow hazard zonation by probabilistic analysis, M T. Woomyeon, Seoul, Korea, International Journal of Innovative Research in Science, Engineering and Technology (IJIRSET), 2, 2381–2390, 2013.
Perla, R., Cheng, T. T., and McClung, D. M.: A two-parameter model of snow-avalanche motion, J. Glaciol., 26, 197–207, 1980.





NHESSD
3, 3509–3541, 2015



Quinn, P., Beven, K., Chevallier, P., and Planchon, O.: The prediction of hillslope flow paths for distributed hydrological modelling using digital terrain models, Hydrol. Process., 5, 59–79, doi:10.1002/hyp.3360050106, 1991.

Rampton, V. N., Ellwood, J. R., and Thomas, R. D.: Distribution and geology of ground ice along the Yukon portion of the Alaska Highway gas pipeline, in: Proceedings of the 4th International Conference on Permafrost, 17–22 July 1983, Fairbanks, Alaska, 4, 1030–1035, 1983.

Rickenmann, D. and Zimmermann, M.: The 1987 debris flows in Switzerland: documentation and analysis, Geomorphology, 8, 175–189, 1993.

Riopel, S., Couture, R., and Tewari, K.: Mapping susceptibility to landslides in a permafrost environment: case study in the Mackenzie Valley, Northwest Territories, GeoTech Event, Ottawa, Canada, 18–21 June, 13 pp, 2006.

Savage, W. and Baun, R.: Instability of steep slopes, in: Debris-Flow Hazards and Related Phenomena, edited by: Matthias, J. and Oldrich, H., Springer, Berlin, Heidelberg, 53–70, 2005.

Soeters, R. and van Westen, C. J.: Slope instability recognition, analysis, and zonation, in: Landslides, Investigation and Mitigation, edited by: Turner, A. K. and Schuster, R. L., Transportation Research Board, National Research Council, Special Report 247, National Academy Press, Washington, DC, 129–177, ISBN 0-309-06151-2, 1996.

Takahashi, T.: Estimation of potential debris flows and their hazardous zones: soft countermeasures for a disaster, Natural Disaster Science, 3, 57–89, 1981.

Tarboton, D. G.: A new method for the determination of flow directions and upslope areas in grid digital elevation models, Water Resour. Res., 33, 309–319, doi:10.1029/96WR03137, 1997.

van Westen, C. J., Castellanos, E., and Kuriakose, S. L.: Spatial data for landslide susceptibility, hazard, and vulnerability assessment: an overview, Eng. Geol., 102, 112–131, 2008.

Yukon Geological Survey: http://www.geology.gov.yk.ca/digital_surficial_data.html (last access: 15 April 2014, 2014.





NHESSD

3, 3509–3541, 2015



**Table 1.** Debris flow parameters and class ratings.

| Permafrost distribution probability ($P$) | Rating | Surficial geology ($G$) unit | Rating | Slope angle (°) ($S1$) | Rating | Slope aspect (°) ($S2$) | Rating |
|---|---|---|---|---|---|---|---|
| 0–0.1 | 0.1 | Colluvium, Tuff | 1.0 | 0–15 | 0.1 | 0–45 | 0.1 |
| 0.1–0.2 | 0.2 | Eolian, Lacustrine (vC, C), Glacio-lacustrine (vC, C) | 0.7 | 15–25 | 0.5 | 45–135 | 0.5 |
| 0.2–0.3 | 0.3 | Till, Drift, Glacio-lacustrine (M) | 0.5 | 25–45 | 1.0 | 135–225 | 1.0 |
| 0.3–0.4 | 0.4 | Glacio-lacustrine (F) | 0.4 | 45–55 | 0.5 | 225–315 | 0.5 |
| 0.4–0.5 | 0.5 | Glaciofluvial | 0.3 | 56–90 | 0.1 | 315–360 | 0.1 |
| 0.5–0.6 | 0.6 | Organics, Alluvium, Rock, Anthropogenic | 0.1 | | | | |
| 0.6–0.7 | 0.7 | | | Proximity to drainage (m) ($D$) | Rating | | |
| 0.7–0.8 | 0.8 | | | 0–50 | 1.0 | | |
| 0.8–0.9 | 0.9 | | | 50–100 | 0.75 | | |
| 0.9–1.0 | 1.0 | | | 100–150 | 0.5 | | |
| | | | | 150–200 | 0.25 | | |
| | | | | > 200 | 0.1 | | |

vC = very course, C = course, M = medium, F = fine.





NHESSD
3, 3509–3541, 2015



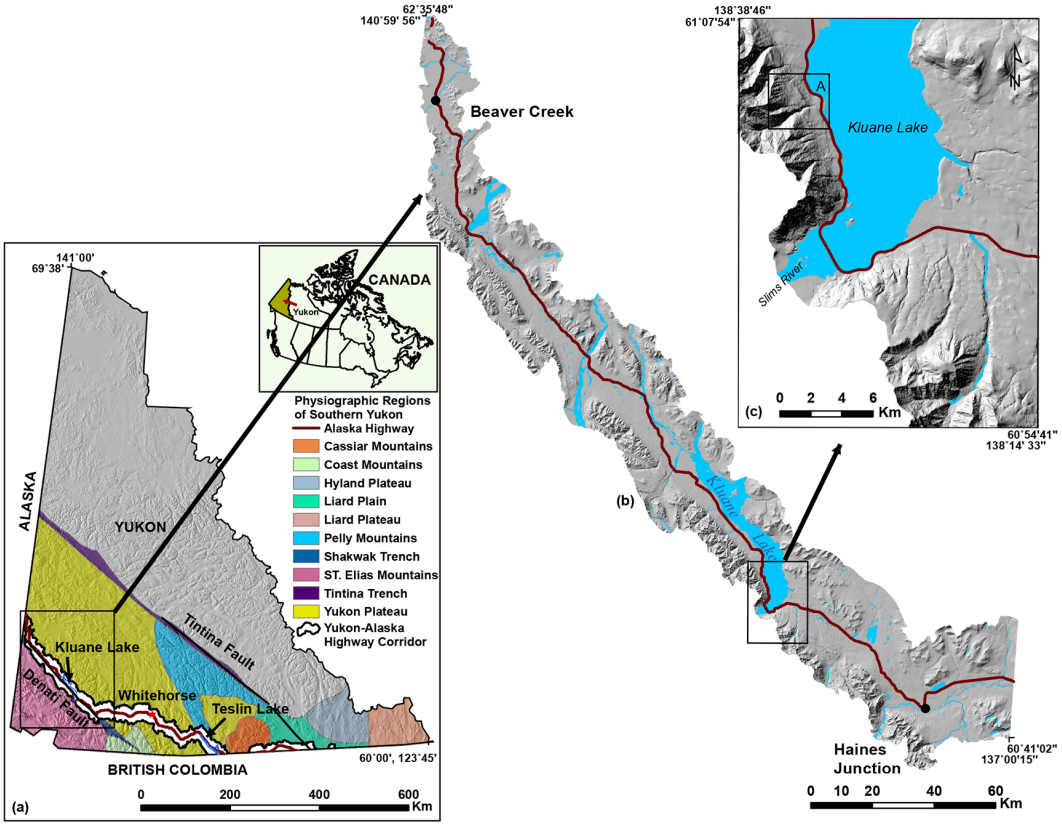


**Figure 1. (a)** Physiographic setting of southern Yukon (modified from Mathews, 1986; Huscroft et al., 2004) and **(b)** northern portion of YAHC where regional debris flow susceptibility mapping was carried out. **(c)** South end of Kluane Lake area where the quantitative susceptibility assessment was performed. Box A in **(c)** shows the location of Fig. 4.





NHESSD
3, 3509–3541, 2015

Debris flow susceptibility mapping along the YAHC

A. Blais-Stevens and P. Behnia



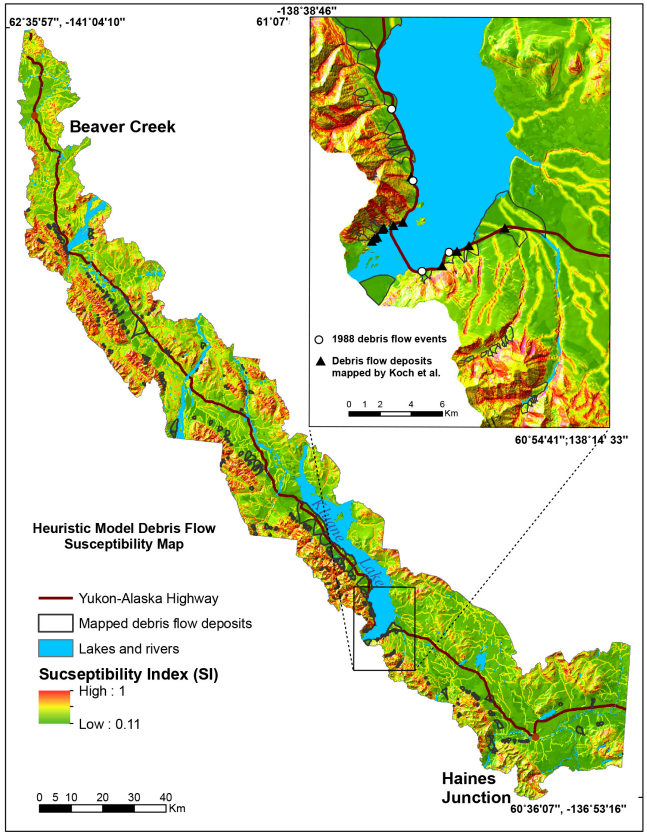


**Figure 2.** Debris flow susceptibility map created using the qualitative heuristic method for the northern part of YAHC (Fig. 1b). Inset map shows south end of Kluane Lake area (Fig. 1c)





NHESSD
3, 3509–3541, 2015



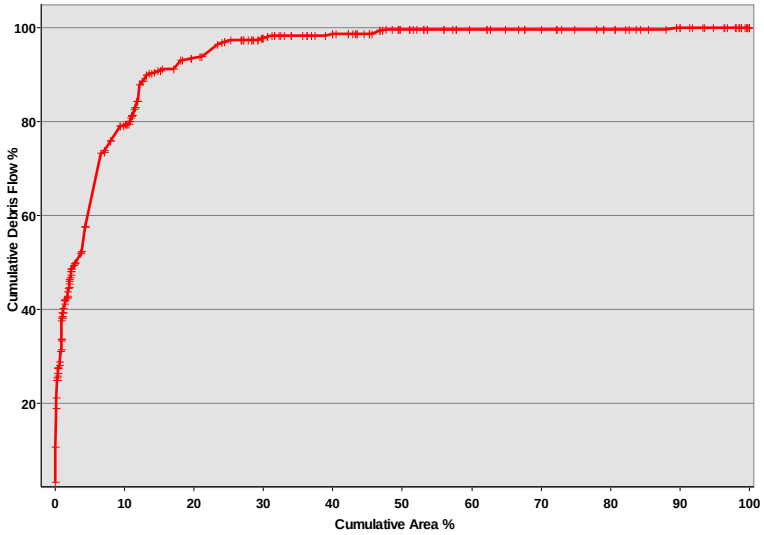


**Figure 3.** Prediction rate of qualitative heuristic debris flow susceptibility map represents a good correlation between debris flow susceptibility and inventory.





NHESSD
3, 3509–3541, 2015



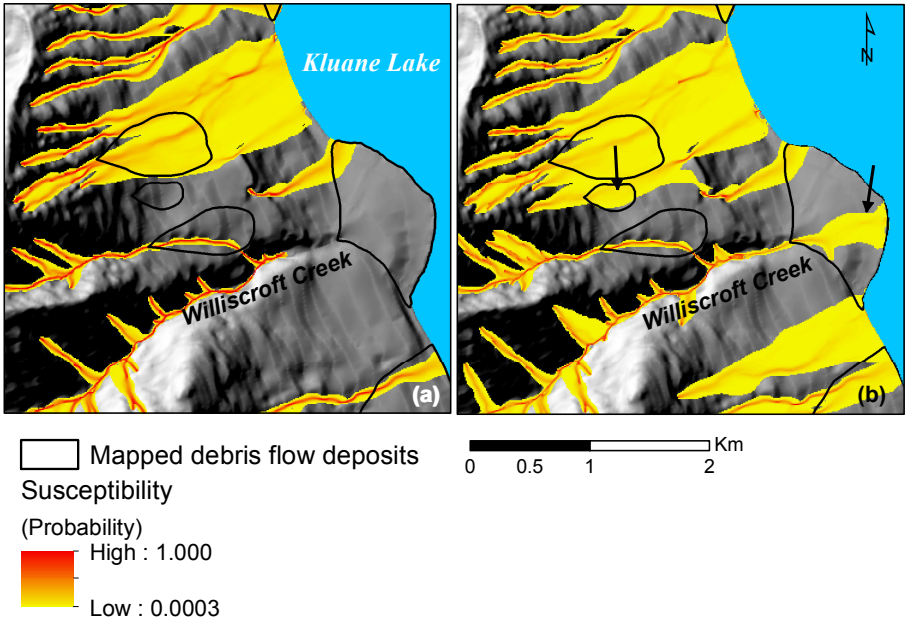


**Figure 4. (a)** The propagation of source areas in and around Williscroft Creek area (box A in Fig. 1) based on the threshold value of $-0.1.5/100\,m^{-1}$, and **(b)** based on the threshold value of $-0.1/100\,m^{-1}$. Note the two debris flow deposits that are captured only in **(b)** are shown with black arrows.





NHESSD
3, 3509–3541, 2015

Debris flow susceptibility mapping along the YAHC

A. Blais-Stevens and P. Behnia



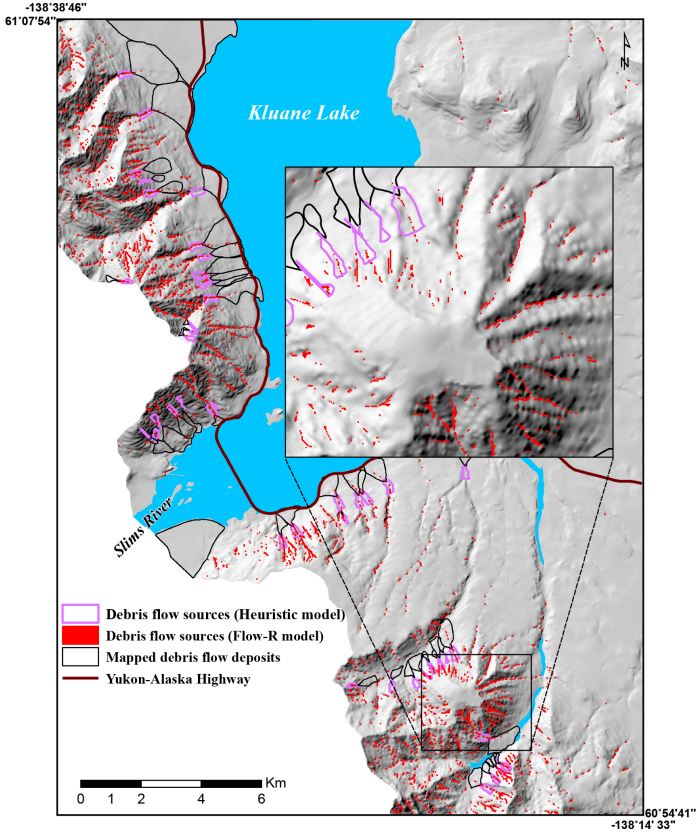


**Figure 5.** Potential debris flow source areas for the south end of Kluane Lake derived by integrating controlling factors. Inset map displays an enlargement of the calculated source areas (red areas; Flow-R) and the assumed potential source areas (purple lines; Heuristic method). Refer to Fig. 1c for location of Fig. 5.





NHESSD
3, 3509–3541, 2015



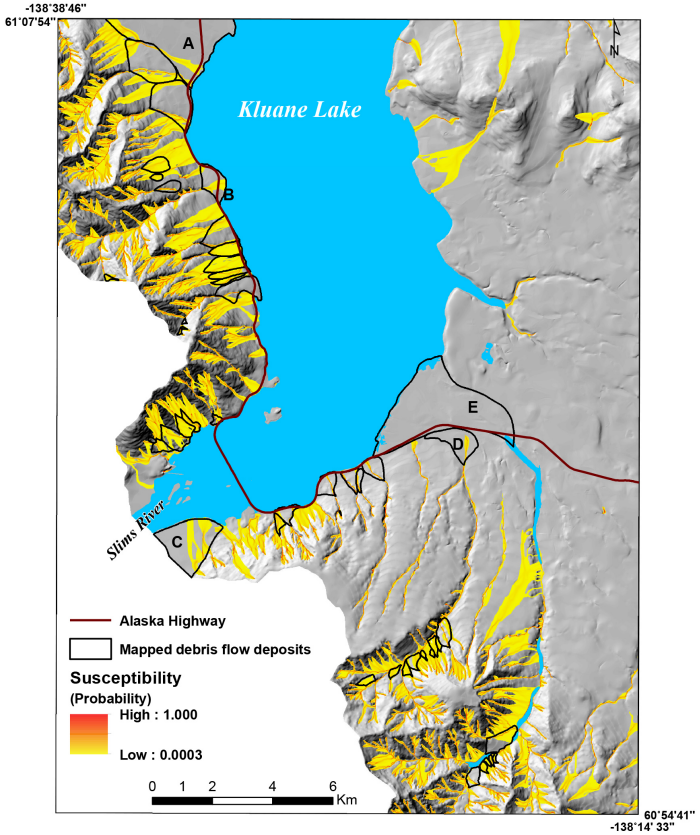


**Figure 6.** Debris flow susceptibility map derived from propagation of source areas using $\omega$ = 150 and $\mu$ = 0.02. Note no propagation reaches debris flow deposit E.





NHESSD
3, 3509–3541, 2015



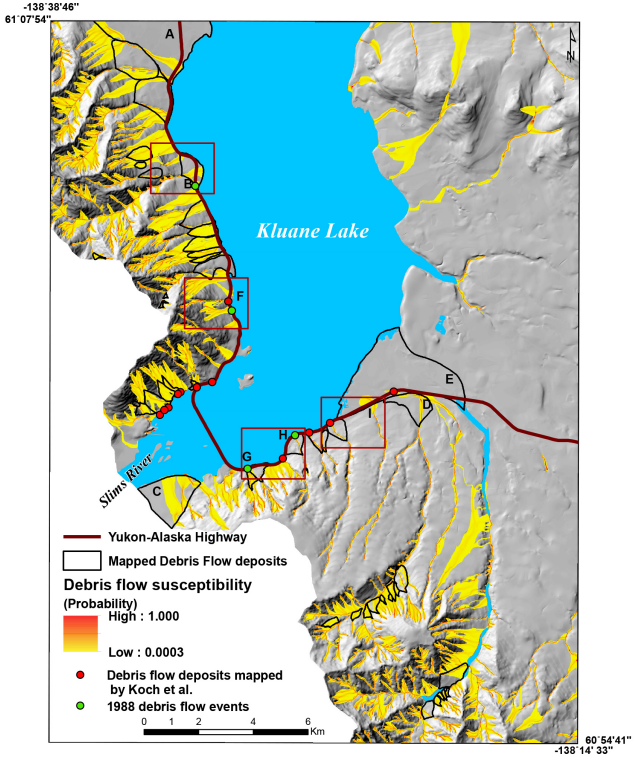


**Figure 7.** Debris flow susceptibility map derived from propagation of source areas using $\omega$ = 600 and $\mu$ = 0.02. Minor propagation is seen reaching the southwest edge of debris flow deposit E. Also note the propagation pattern in C, D and I. Debris flow susceptibility displays a good correlation with the mapped debris flow deposits (black lines from Blais-Stevens, 2010a), the documented 1988 event from Evans and Clague (1989; green dots) and from the detailed study from Koch et al. (2014; red dots).





NHESSD
3, 3509–3541, 2015



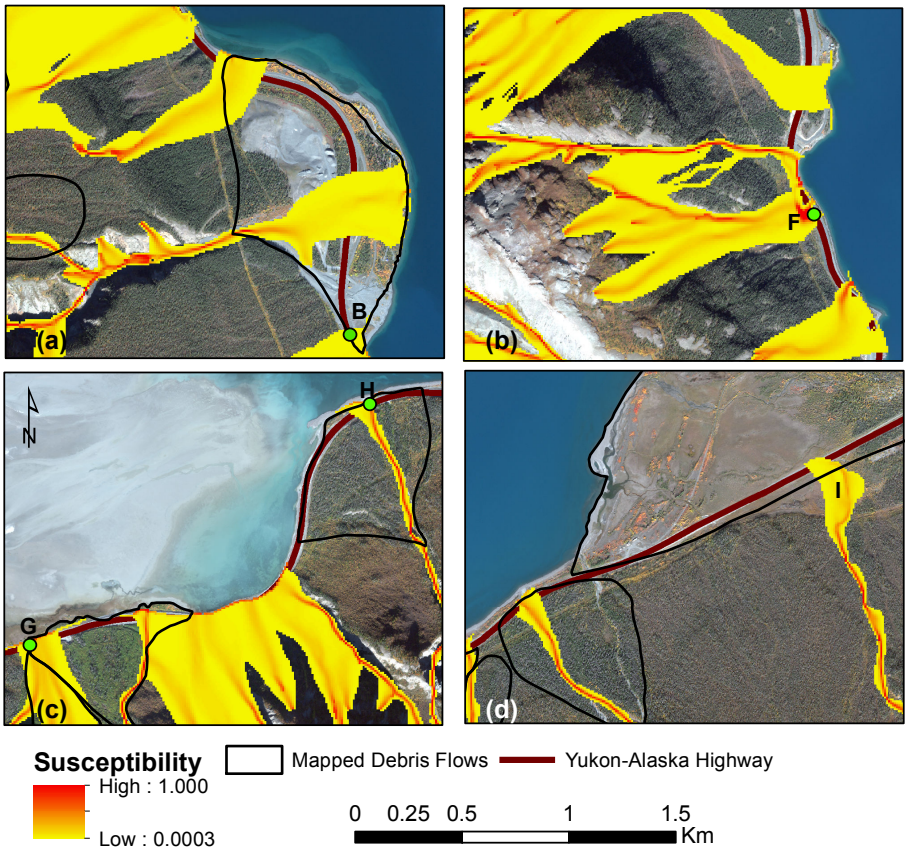


**Figure 8. (a–c)** The susceptibility map overlaid on WorldView2 satellite imagery (2010) shows the location of debris flow deposits which blocked the highway in 1988 (B, F, and G) and in 1967 (H). **(d)** shows a potential debris flow (I) that could reach the highway.





NHESSD
3, 3509–3541, 2015



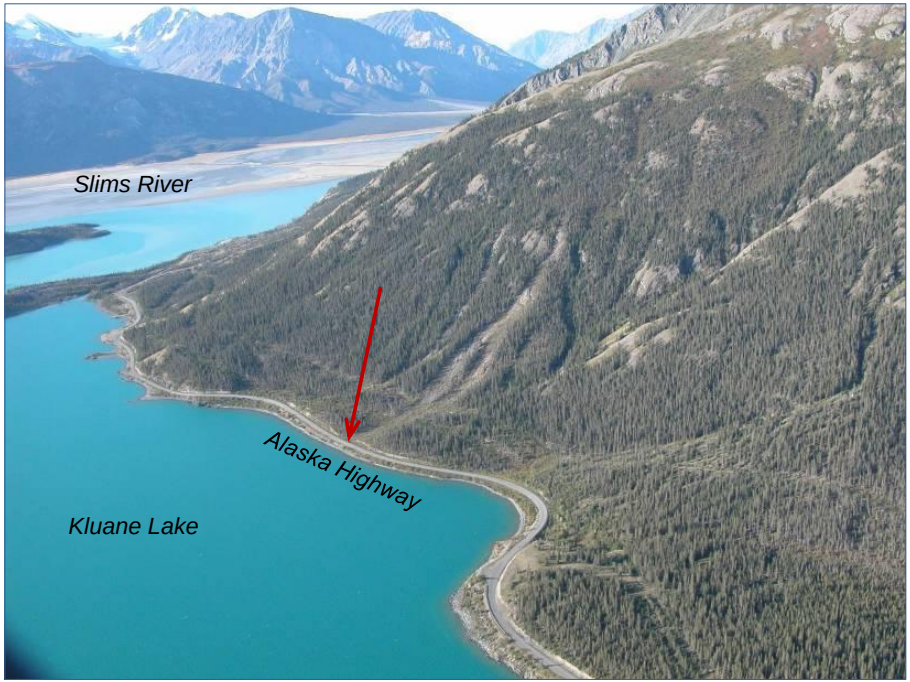


**Figure 9.** Oblique photo of debris flow channels at Horseshoe Bay, southwestern end of Kluane Lake (photo by C. Huscroft). During the 1988 storm event, debris flow deposits blocked the Alaska Highway (e.g., red arrow) for up to seven days (Evans and Clague, 1989). Site F in Figs. 7 and 8b).





NHESSD
3, 3509–3541, 2015